

**A COMPARATIVE STUDY OF MICROSTRUCTURAL AND MAGNETIC  
PROPERTIES OF LSMO: NiFe<sub>2</sub>O<sub>4</sub> NANOCOMPOSITES PREPARED BY  
MICROWAVE AND SOLID STATE ROUTE**

**A THESIS SUBMITTED IN PARTIAL FULFILLMENT  
OF THE REQUIREMENTS FOR THE DEGREE OF**

**Bachelor of Technology  
in  
Ceramic Engineering**

**By  
NAMITHA V**



**Department of Ceramic Engineering  
National Institute of Technology  
Rourkela  
2011**

**A COMPARATIVE STUDY OF MICROSTRUCTURAL AND MAGNETIC  
PROPERTIES OF LSMO: NiFe<sub>2</sub>O<sub>4</sub> NANOCOMPOSITES PREPARED BY  
MICROWAVE AND SOLID STATE ROUTE**

A THESIS SUBMITTED IN PARTIAL FULFILLMENT  
OF THE REQUIREMENTS FOR THE DEGREE OF

**Bachelor of Technology  
in  
Ceramic Engineering**

By  
**NAMITHA V.**

Under the Guidance of  
**Prof Bibhuti B. Nayak**



**Department of Ceramic Engineering  
National Institute of Technology  
Rourkela  
2011**



**National Institute of Technology**

**Rourkela**

**CERTIFICATE**

This is to certify that this thesis entitled, “A COMPARATIVE STUDY OF MICROSTRUCTURAL AND MAGNETIC PROPERTIES OF LSMO:  $\text{NiFe}_2\text{O}_4$  NANOCOMPOSITES PREPARED BY MICROWAVE AND SOLID STATE ROUTE” submitted by Miss NAMITHA .V in partial fulfillments for the requirements for the award of Bachelor of Technology Degree in Ceramic Engineering at National Institute of Technology, Rourkela is an authentic work carried out by him under my guidance.

To the best of my knowledge, the matter embodied in the thesis has not been submitted to any other University / Institute for the award of any Degree or Diploma.

Date:

Prof Bibhuti B Nayak  
Associate Professor  
Department of Ceramic Engineering,  
National Institute of Technology,  
Rourkela- 769 008

## **ACKNOWLEDGEMENTS**

The completion of this project stems from the efforts of many people, their guidance and support. I would like to thank Prof Bibhuthi B. Nayak for helping me with the fundamentals and advanced concepts as well. He has also guided me with his valuable advices which have helped me complete my project on time.

The role of PhD and M.Tech scholars can't also be neglected. Special thanks to Subrat sir and Naidya sir for providing me with the instruments needed to work in the lab and also teaching me how to use those instruments.

I am grateful to Prof S.K Prathihar for helping me with the DSC/TG characterization of my samples. Special thanks to Mr Rajesh Pattnaik for doing SEM of my samples and MR Sushil Sahoo for XRD.

Lastly I would like to thank my batch mates namely Rahul Mohanty, Deepak Patgiri and Pashupati Nath Mishra for creating a friendly environment. They were with me when I nervously waited for the experimental results and also helped me in giving some useful impetus at times.

5<sup>th</sup> May, 2011

NAMITHA .V

# CONTENTS

	Page No.
<i>Abstract</i>	<i>i</i>
<i>List of Figures</i>	<i>ii</i>
<i>List of Tables</i>	<i>iii</i>
<b>Chapter 1</b>	
<b>GENERAL INTRODUCTION</b>	1-2
1.1 Introduction	2
1.2 Outline of the report	2
<b>Chapter 2</b>	
<b>LITERATURE REVIEW</b>	3-6
2.1 Structure and properties of manganites	4
2.2 Structure and properties of ferrites	4
2.3 Microwave synthesis of manganite ferrite composite	5
2.4 Objectives	6
<b>Chapter 3</b>	
<b>EXPERIMENTAL WORK</b>	7-11
3.1 Synthesis of pure LSMO and NiFe <sub>2</sub> O <sub>4</sub>	8
3.1.1 <i>Experimental setup</i>	8
3.2 Microwave assisted in-situ synthesis of LSMO: NiFe <sub>2</sub> O <sub>4</sub> composites	9
3.2.1 <i>Experimental setup</i>	9
3.3 Synthesis of LSMO: NiFe <sub>2</sub> O <sub>4</sub> composites by solid-state route	10
3.3.1 <i>Experimental setup</i>	10
3.4 General characterization	10
<b>Chapter 4</b>	
<b>RESULTS AND DISCUSSIONS</b>	12-25
4.1 Characterization of pure LSMO and NiFe <sub>2</sub> O <sub>4</sub>	13
4.1.1 Thermal	13
4.1.2 Structure and microstructure	14
4.1.3 Density	15
4.1.4 Magnetic hysteresis loop	16
4.1.5 Remarks	16
4.2 Characterization of in-situ LSMO: NiFe <sub>2</sub> O <sub>4</sub> composites	17
4.2.1 Thermal	17
4.2.2 Structure and microstructure	18
4.2.3 Density	20
4.2.4 Magnetic hysteresis loop	20
4.2.5 Remarks	21
4.3 Characterization of LSMO: NiFe <sub>2</sub> O <sub>4</sub> composites by solid-state route	21
4.3.1 Structure and microstructure	21
4.3.2 Density	23
4.3.3 Magnetic hysteresis loop	24
4.3.4 Remarks	25
<b>Chapter 5</b>	
<b>CONCLUSIONS</b>	26-27
<b>References</b>	28

## **Abstract**

The present work deals with the preparation and the characterization of nickel ferrite and lanthanum strontium manganese oxide composites. The composites were prepared in two different routes i.e. in-situ route and solid state routes. The composites were prepared with three different ratios of the phases in each individual route. The ratios were 20LSMO:80NFO, 40LSMO:60NFO and 50LSMO:50NFO. The composites synthesized were subjected to characterization by XRD, SEM, DSC/TG and M-H curve. The values obtained from the composites prepared from the in-situ method were compared with the values obtained from simple solid state methods. There were differences in the porosity values of the two methods. All the samples are characterized using XRD and found to be rhombohedral LSMO and cubic NFO phases. The crystallite size was found to be less than 50 nm. From SEM it was seen that the porosity of in-situ process samples is more than that of solid state process. It was observed that as the concentration of the NFO in the samples increased the magnetic properties also improved. The saturation magnetization (Ms) and coercivity (Hc) value for NFO comes out to be 52.7 emu/g and 74 Oe.

## List of Figures

	<b>Page No</b>
Fig.4.1.1 DSC-TG of as-prepared (a) LSMO and (b) NFO	13
Fig.4.1.2 XRD patterns of (a) LSMO (b) NFO sintered at 1200 °C; (c) SE image of LSMO (d) BSE image of LSMO	14-15
Fig.4.1.3 M-H curve (a) NFO.	16
Fig.4.2.1 DSC-TG curve of (a) 50:50 (b) 40:60(c) 20:80 in-situ synthesized composites	17
Fig.4.2.2 Fig 4.2.2: XRD pattern of (a) 50:50, (b) 40:60 (c) 20:80 images; (c), (d) shows the secondary electron image and backscattered image of in-situ synthesized 40:60(LSMO: NFO) composite; also the EDAX.	18
Fig.4.2.3 MH loop (a) 50 LSMO: 50 NFO, (b) 40 LSMO: 60 NFO, and (d) 20 LSMO: 80 NFO samples.	20
Fig 4.3.1 pattern of (a) 50 LSMOs: 50NFO, (b) 40 LSMO: 60 NFO and (c) 20 LSMO: 80 NFO; (c) 60:40(Secondary Electron image), (d) 60:40 (backscattered electron image) showing EDAX	21-22
Fig 4.3.2 Hysteresis loop (a) 50:50, (b) 40:60, and (d) 20:80	24

## List of Tables

		<b>Page No.</b>
Table 3.1	Shows the amount of salts used for synthesis of samples	9
Table 3.2:	Shows the weight of LSMO and NFO used for the synthesis of pallets through solid route.	10
Table 4.1	Shows the values of Bulk density and apparent porosity of in-situ samples.	20
Table 4.2	Table 4. 3: Bulk density and apparent porosity of solid route synthesized samples	23
Table 4.3	Bulk density and apparent porosity synthesized samples	23
Table 4.4	shows the values for Coercive Field ( $O_e$ ), Remanent magnetization ( $M_r$ ) in emu/g, Saturation magnetization ( $M_s$ ) in emu/g in different composition of LSMO and NFO, prepared by different routes	25



# Chapter 1

## GENERAL INTRODUCTION

## *1.1 Introduction*

Magnetic and electrical transitions at the same time for some particular composition ranges of LSMO have been an interesting area of research in the recent years. They change their properties from paramagnetic to ferromagnetic and undergo a metallic transition during cooling. If an external magnetic field is applied, then this transition will show a significant increase in conductivity. This is called negative magnetoresistance [1].

Close to the transition temperature these oxides show a significant decrease in their magneto-resistance values. This is a very useful phenomenon in storage applications. There is a decrease in grain size, increase in magneto-resistance values and a decrease in substitution doping when low fields are applied [1].

The work presented in this paper deals with a composite of Ni-ferrite and La-Sr-manganite which has been synthesized by microwave assisted in situ and solid state method both. With the help of a microwave assisted synthesis, uniformity in the distribution of the two phases can be got [2].

The LSMO/LCMO nanocomposites will not show any electrical conductivity but will show magnetic properties along with ferrites when the temperature is above their transition temperature. When the temperature is lesser than its transition temperature the composite shows colossal MR behaviour and this property makes it a very useful component in many magnetic devices. [3].

## *1.2 Outline of the report*

The present chapter provides a brief introduction to the topic under concern. The second chapter reviews the already published papers in this area and this section is concluded by the objective of the present work. The third chapter explains the different experimental techniques used. Chapter number 4 analyses and describes in detail the results obtained and reasons out the obtained results. The last section is conclusions which sums up the work and enlists the conclusion drawn from the results obtained.

# Chapter 2

## LITERATURE REVIEW

## *2.1 Structure and properties of manganites*

Manganites have a property of colossal Magnetoresistance which has made them a very important topic of research. Curie temperature LSMO is 365K. Below the Curie temperature a high value of MR was observed but on increasing the temperature monotonically MR value showed a decrease. [4].

Compounds which are rich in  $\text{Mn}^{3+}$  are doped with divalent atoms which produce both  $\text{Mn}^{3+}$  and  $\text{Mn}^{4+}$  which are important in producing the double exchange effect. Electrons are exchanged from  $\text{Mn}^{3+}$  to  $\text{Mn}^{4+}$  in the presence of oxygen when the two ions have parallel core spin. This is called double exchange effect. [5].

The CMR effects observed in polycrystalline ceramic bulk can be classified into two categories of Magnetoresistance (MR) namely intrinsic MR and extrinsic MR. The extrinsic MR can be observed in manganites. The extrinsic MR effect is because of the inter grain effect for which higher MR was observed for temperature below  $T_c$ .

## *2.2 Structure and properties of ferrites*

Ferrites are known for their excellent dielectric properties. The crystalline Ni-ferrite has an inverse spinel structure at room temperature. The formula of spinel structure is  $\text{AB}_2\text{O}_4$ , which is a cubic closed-packed oxygen arrangement, inside which the cations reside inside the tetrahedral sites [A] and also inside the octahedral [B] sites [6].

## *2.3 Microwave synthesis of manganite ferrite composite*

The magnetic behavior of La-Sr-Mn-O was studied by Yan et al. [4] and Huang et al. [3]. Magnetically coupling along with the LSMO grains, FM influences the transport properties. For  $x \geq 0.05$  M NF, there is no electrical transition and transport is mainly dominated by a typical semiconducting/insulating behavior. This behavior can be attributed to that Ni and Fe substitute the Mn site of LSMO. The MR increases values show an increase with a decrease in temperature for a 0.01M NFO composite.

Nayak et al. [2] has synthesized the composite of LCMO and NF by microwave refluxing method. Uniformly distributed composite phases were obtained in this technique.

The double exchange process depends on many external factors and is affected by the chemical composition. In LCMO the double exchange process is caused by  $\text{Mn}^{3+}-\text{O}^{2-}-\text{Mn}^{4+}$  ions. Studies show that the double exchange process is affected by addition of NF to LCMO. [7].

Other work in the area of study of magnetic properties include the  $\text{La}_{2/3}\text{Ca}_{1/3}\text{MnO}_3$  with alumina composite which proved to show an increase in intergranular magnetoresistance by three times [8].  $\text{La}_{0.67}\text{Ca}_{0.33}\text{MnO}_3 + x\% \text{V}_2\text{O}_5$  ( $x = 0, 2, 5, 15$  and  $30$ ) composites, showed a decrease in metal-insulator transitions at  $T = T_p$ , except for the one with  $x = 30\%$  with increasing  $\text{V}_2\text{O}_5$  concentration. [9].  $\text{La}_{0.7}\text{Pb}_{0.3}\text{MnO}_3 + x \text{Ag}$  ( $x = 0-20$  wt %) nanocomposites, with increasing Ag concentration showed an increase in conductivity ( $\sigma$ ) and metal-insulator transition temperature ( $T_p$ ) with a decrease in magnetization. [10].

The  $\text{La}_{0.67}\text{Sr}_{0.33}\text{MnO}_3/\text{BaFe}_{11.3}(\text{ZnSn})_{0.7}\text{O}_{19}$  (LSMO/BaM) were prepared and the microstructural, magnetic, and magnetoresistive (MR) were studied [11]. Magnetic studies on K-doped  $\text{La}_{1-x}\text{Ca}_x\text{K}_y\text{MnO}_3$  also have been reported [12].  $(\text{La}_{1-x}\text{Ca}_x\text{MnO}_3)_{1-y}(\text{ZrO}_2)_y$  composites show higher magnitude of MR compared to pure LCMO. [13]

Studies that show the electronic and magnetic properties of Mn (III)-rich manganites are better than that of Mn (IV)-rich manganites have also been reported. [14]. There are studies on the magnetic properties of perovskite compounds with the help of x-ray diffraction and neutron electron diffraction methods. [15]. But in the present work, magnetic properties are studied with the help of M-H curve.

## *2.4 Objectives*

1. In the present work, composites with varying ratio of nickel ferrite and lanthanum strontium manganese oxide were prepared. The ratios were 80:20, 60:40 and 50:50 for NFO and LSMO respectively. The composites were prepared by two routes .One is the microwave route and the other is the solid state route.
2. The prepared samples were subjected to XRD, SEM, DSC-TG and M-H curve characterization and the values obtained from the composites synthesized by microwave route were compared with that obtained from solid state route.

# Chapter 3

## EXPERIMENTAL WORK

### 3.1 Synthesis of pure LSMO and $\text{NiFe}_2\text{O}_4$

#### 3.1.1 Experimental Setup

##### Synthesis of single phase nickel ferrite:-

1. Weights of the salts required to prepare a 7g batch pure nickel ferrite was calculated.

The weights were:-

a. Nickel chloride = 10.1415 grams

b. Ferric chloride = 13.840 grams.

2. 1,2 ethanediol (100ml) was poured into a beaker and all the above salts were dissolved in it one by one accompanied by heating and stirring. This is solution A.

3. A KOH solution was prepared by weighing 20 grams of solid KOH and dissolving it in 1,2 ethanediol(100ml). This is solution B.

4. Solution B is added dropwise to solution A so that the pH increases to about 12 or 13. A thick gel was formed.

5. Refluxing of the precipitate is then done in a microwave oven (time- 60 min).

6. After the refluxing process is complete the precipitate is washed till the pH reduces to 7. Then the precipitate is oven dried and ground with the help of a motor pestle to a fine powder.

7. The ground powder was calcined at for 2hrs in a furnace at a temperature of 1100 degree celcius.

##### Synthesis of single phase lanthanum strontium manganese oxide:-

1. Weights of the salts required to prepare a 7g batch pure lanthanum strontium manganese oxide was calculated.

The weights were:-

a. Lanthanum acetate = 10.12 grams

b. Strontium chloride = 2.3 grams.

c. Manganese acetate = 10.756 grams

2. 1,2 ethanediol (100ml) was poured into a beaker and all the above salts were dissolved in it one by one accompanied by heating and stirring. This is solution A.



3. A KOH solution was prepared by weighing 20 grams of solid KOH and dissolving it in 1,2 ethanediol(100ml). This is solution B.
4. Solution B is added drop wise to solution A so that the pH increases to about 12 or 13. A thick gel was formed.
- 5.Refluxing of the precipitate is then done in a microwave oven (time- 60 min).
6. After the refluxing process is complete the precipitate is washed till the pH reduces to 7. Then the precipitate is oven dried and ground with the help of a motor pestle to a fine powder.
7. The ground powder was calcined at for 2hrs in a furnace at a temperature of 1100 degree celcius.

### **3.2 Microwave assisted in-situ synthesis of LSMO: NiFe<sub>2</sub>O<sub>4</sub> composites**

#### **3.2.1 Experimental Setup**

- 1.Weights of the salts required to prepare a 7g batch was calculated. The table below gives the calculated weights for different compositions:-
2. 1,2 ethanediol (100ml) was poured into a beaker and all the above salts were dissolved in it one by one accompanied by heating and stirring. This is solution A.
3. A KOH solution was prepared by weighing 20 grams of solid KOH and dissolving it in 1,2 ethanediol(100ml). This is solution B.
4. Solution B is added drop wise to solution A so that the pH increases to about 12 or 13. A thick gel was formed.
- 5.Refluxing of the precipitate is then done in a microwave oven (time- 60 min).
6. After the refluxing process is complete the precipitate is washed till the pH reduces to 7. Then the precipitate is oven dried and ground with the help of a motor pestle to a fine powder.
7. The ground powder was calcined at for 2hrs in a furnace at a temperature of 1100 degree Celsius.

Table 3.1: Shows the amount of salts used for synthesis of samples.

LSMO: NFO	Nickel chloride(g)	Ferric chloride(g)	Lanthanum acetate(g)	Strontium chloride(g)	Manganese acetate(g)
50:50	3.6227	4.9441	3.2271	1.3408	3.7351
40:60	4.278	5.839	1.074	0.453	1.274
20:80	2.371	3.244	0.529	0.22	0.612

### 3.3 Synthesis of LSMO: NiFe<sub>2</sub>O<sub>4</sub> composites by solid-state route

#### 3.3.1 Experimental Setup

The LSMO and NFO pure powders were taken in a mortar pestle and ground to a fine powder. The ratio required according to the required composition was taken according to the table given below.

Table 3.2: Shows the weight of LSMO and NFO used for the synthesis of pellets through solid route.

Ratio	NFO(g)	LSMO(g)
80: 20	0.48	0.12
50: 50	0.3	0.3
60: 40	0.36	0.24

#### **Preparation of pellets and sintering:-**

1. 0.6g of the powder to be made into pellets is taken in a mortar pestle and PVA is added to it. The powder is pressed and sintered at 1200 degrees for 2 hours in a raising heart furnace.

#### 3.4 General characterization

##### *Thermal (DSC-TG)*

The thermo gravimetric analysis and differential scanning calorimeter was done using a (NETZCH STA 449 C, Germany). The characterization were done using a heating rate of 10°C/min from temperature starting from 30 °C to 1000 °C.

##### *Structural (XRD)*

The XRD graphs were obtained from the Phillips PANalytical (model number PW 3040, Netherland) diffractometer with a Cu K $\alpha$  radiation ( $\lambda=0.15406$  nm) with a graphite secondary beam monochromatic; the intensities were studied from 20° to 80° and the step rate used was 0.04/sec and a measuring time equal to 25mins. Debye-Scherrer formulae has been applied to calculate the values of the crystallite size.

### *Microstructural (SEM with EDAX)*

The microstructural study was done using a Scanning Electron Microscope (model-JEOL JSM 6480LV). With the help of the Secondary electron images the topology of the surface was studied and with the help of backscattered electrons images the discrimination in mass was studied. From EDAX chemical analysis was done.

### *Density Measurement*

The porosity and density of sintered pellets were calculated using the formula B.D(bulk density) =  $\frac{D}{W-S} * 0.81$ , and A.P (apparent porosity) =  $\frac{W-D}{W-S} * 100$  for percentage.

### *Magnetic hysteresis loop*

With the help of a PULSE FIELD HYSTERESIS LOOP TRACER of MAGNETA (MUMBAI), the MH loop of all the sintered pellets was obtained.

The pellets were placed one by one inside the sample holder the M-H loops for each individual sample

The following data was obtained from the M-H loop:-

- 1)  $O_c$ -Coercive Field
- 2)  $M_s$ -Saturation magnetization(emu/g)
- 3)  $M_r$ -Remanent magnetization(emu/g)

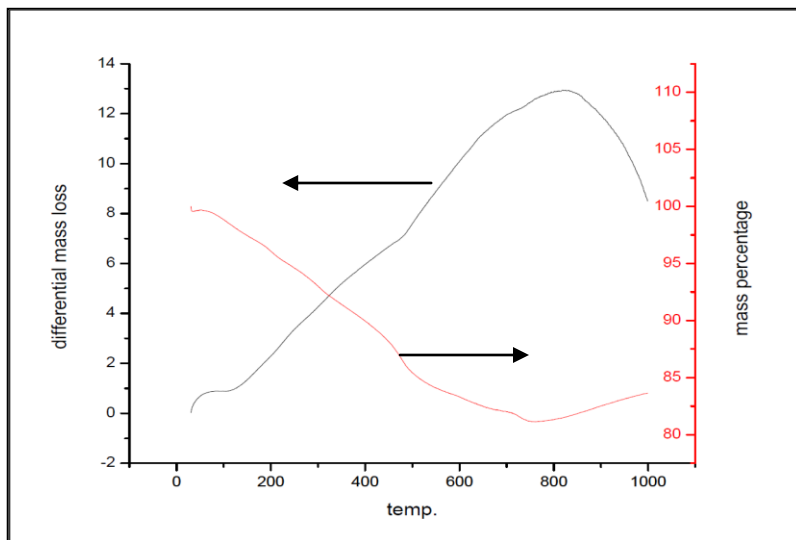
# Chapter 4

## RESULTS AND DISCUSSION

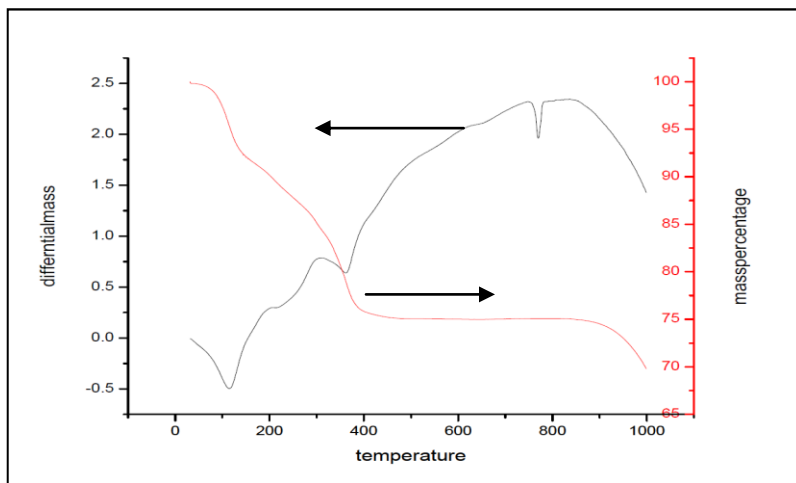
## 4.1 Characterization of pure LSMO and $\text{NiFe}_2\text{O}_4$

### 4.1.1 Thermal

In the figures 4.1.1 (a) and (b) shows the DSC-TG profiles of pure LSMO and NFO powders,



(a)



(b)

Fig 4.1.1: DSC-TG of as-prepared (a) LSMO and (b) NFO.

Because of the crystallization temperature of LSMO or NFO there is a broad exothermic peak approximately from 600 to 1000 degree and endothermic peaks approximately ranging from 110 to 400 degrees in the DSC plot. There was weight loss observed. The weight loss was due to the removal and decrease of absorbed water. For LSMO, two different regions (30-450 °C and 450-800 °C) of weight loss and weight gain is seen at 800 °C. Similar weight losses were seen in the NFO samples.

#### 4.1.2 Structure and microstructure

The presence of phases and crystallite size were calculated from the X-ray diffraction pattern. Figures 4.1.2 (a) and (b) show the XRD of LSMO and NFO samples which have been sintered.

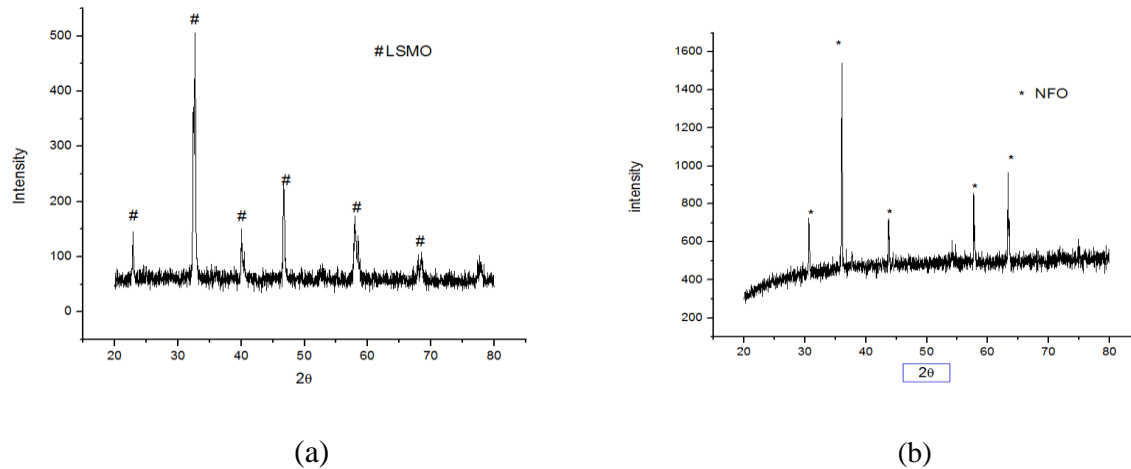
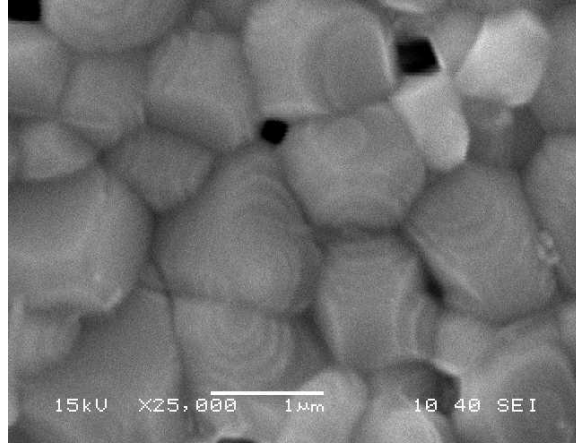


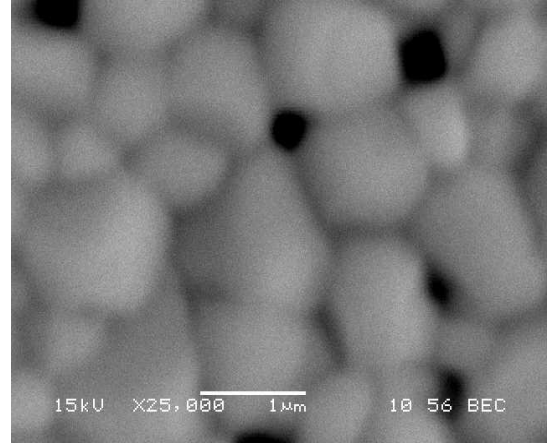
Fig 4.1.2: XRD patterns of (a) LSMO (b) NFO sintered at 1200 °C.

With the help of the JCPDS files (47-0444 for LSMO and 03-0875 for NFO) the phases present were confirmed to be LSMO and NFO, with LSMO having a rhombohedral structure with crystallite size 30nm and NFO having a cubic structure with crystallite structure 55nm.

The particle size, agglomeration and shape of the sintered pellets can be got from the SEM analysis. Figure 4.1.2 (c) and (d) show the SE and BSE images which are taken for LSMO sintered samples.



(c)



(d)

Fig 4.1.2: (c) SE image of LSMO (d) BSE image of LSMO.

From the BSE-image, it can be seen that there is no secondary phase present in this sample. This shows that the sample is pure LSMO. A layer or wavy type of structure can be seen from the above image.

#### **4.1.3 Density**

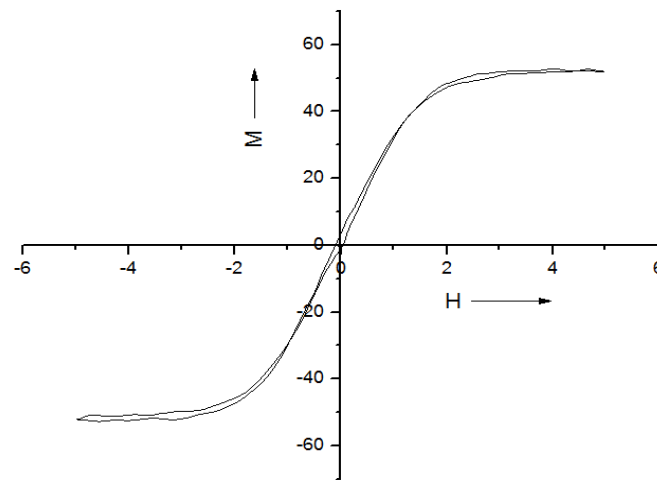
The bulk density(B.D) and apparent porosity(A.P) of sintered LSMO pallets were obtained as 3.76 g/cm<sup>3</sup> and 25.07% respectively.

The bulk density (B.D) and apparent porosity(A.P) of sintered NFO pallets were obtained as 4.27 g/cm<sup>3</sup> and 32.79% respectively.

The bulk density(B.D) and apparent porosity(A.P) of NFO and LSMO samples are given in Table 4.3.

#### 4.1.4 Magnetic hysteresis loop

Fig.4.1.3 shows room temperature MH loop of NFO sintered pellets.



(a)

Fig 4.1.3: M-H curve (a) NFO.

Saturation magnetization and coercivity value come out as 52.7 emu/g and 74 Oe, respectively. NFO sample belongs to soft magnet and the M-H loop of pure LSMO could not be observed due to the low magnetization and magnetic properties of LSMO at room temperature.

#### 4.1.5 Remarks

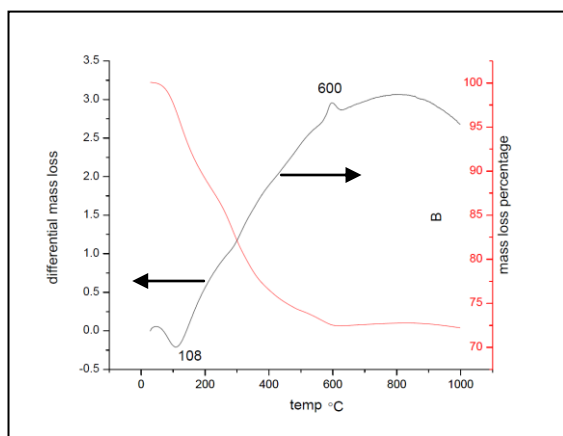
Phase pure LSMO and NFO were synthesized. There was no magnetic behavior observed by LSMO at the room temperature. But NFO showed magnetic behavior and was a soft magnet. Crystallite size of LSMO is 30nm and NFO 55nm. LSMO particles are smaller in size.



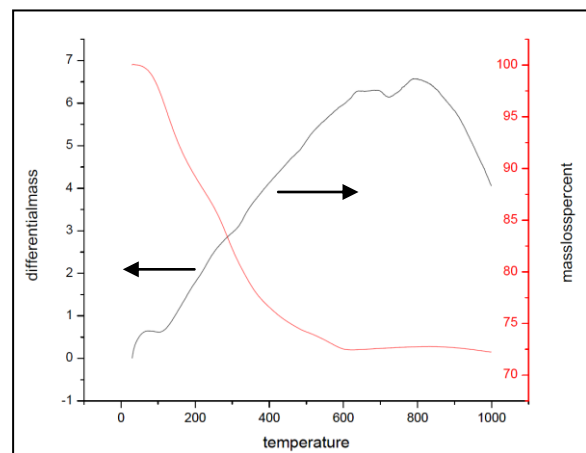
## 4.2 Characterization of in-situ LSMO: NiFe<sub>2</sub>O<sub>4</sub> composites

### 4.2.1 Thermal

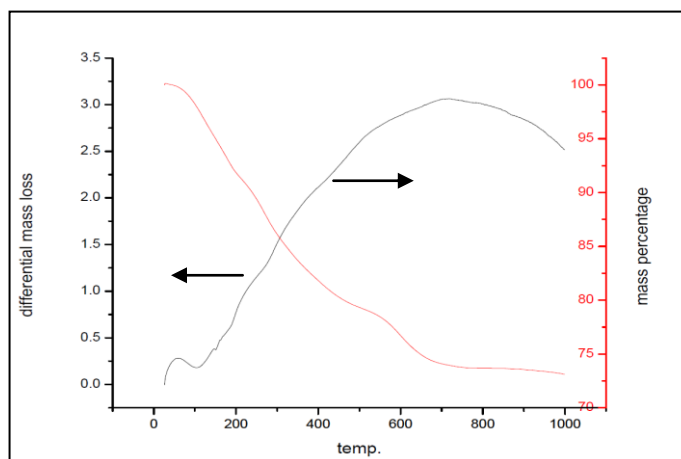
In figures 4.2.1 (a), (b) and (c) are shown the DSC-TG profiles of the composite of LSMO and NFO with ratios 50:50, 40:60 and 20:80 respectively; in-situ synthesized and sintered for 2hrs at 1200 °C .



(a)



(b)



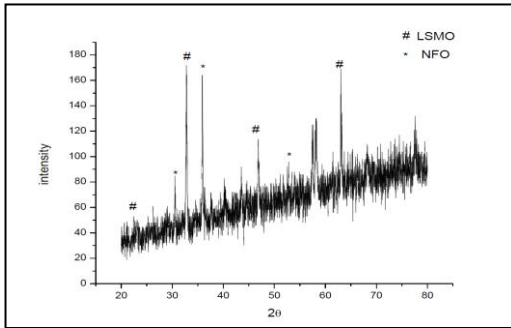
(c)

Fig 4.2.1: DSC-TG curve of (a) 50:50 (b) 40:60(c) 20:80 in-situ synthesized composites.

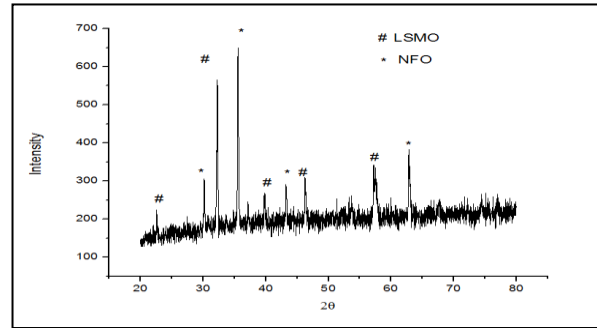
Because of the crystallization temperature of LSMO or NFO there is a broad exothermic peak approximately from 600 to 1000 degree and endothermic peaks approximately ranging from 110 to 400 degrees in the DSC plot. There was weight loss observed. The weight loss was due to the removal and decrease of absorbed water. For 50:50(LSMO: NFO), 40:60(LSMO: NFO), and 20:80(LSMO: NFO), two different regions (30-450 °C and 450-800 °C) of weight.

#### 4.2.2 Structure and microstructure

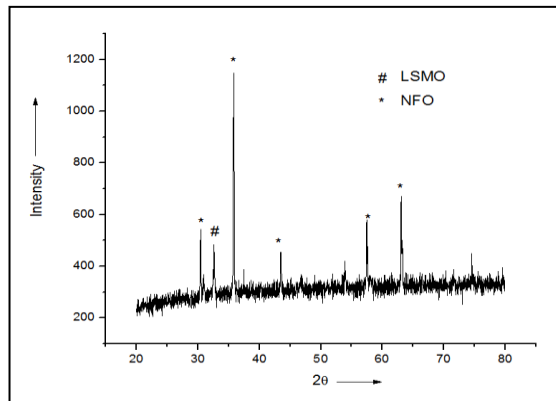
The presence of phases and the crystallite size was calculated from the X-ray diffraction pattern. Figures 4.2.2 (a), (b),(c) shows the XRD graphs of in-situ synthesized composites with composition 50:50 (LSMO: NFO) 40:60(LSMO:NFO) and 20:80 (LSMO: NFO) respectively. All the peaks are identified to either NFO or LSMO without impurities.



(a)



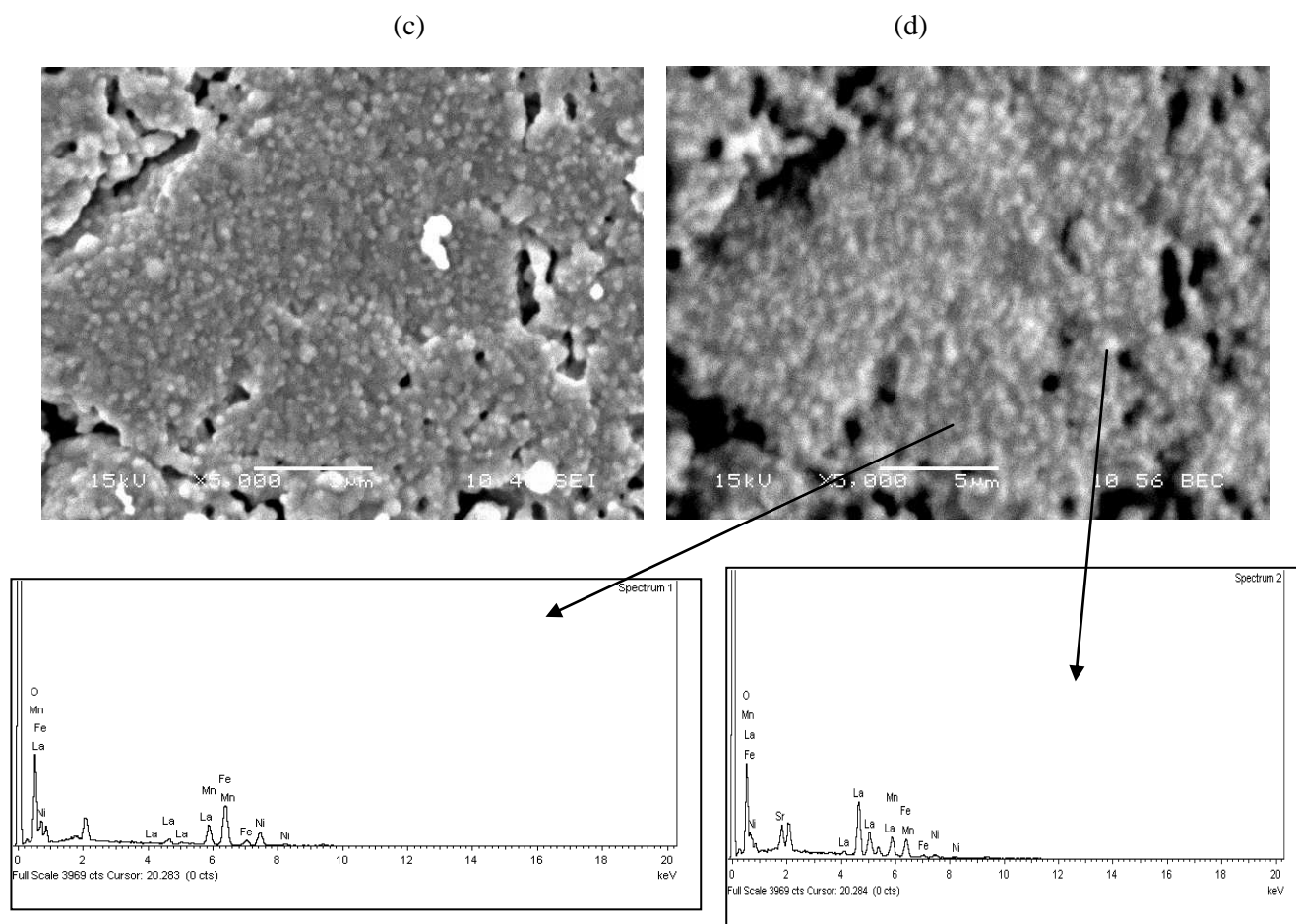
(b)



(c)

Fig 4.2.2: XRD pattern of (a) 50:50, (b) 40:60 (c) 20:80 images

Figures 4.2.2 (c), (d) shows the secondary electron image and backscattered image of in-situ synthesized 80:20(LSMO: NFO) composite.



Figures 4.2.2 (c), (d) shows the secondary electron image and backscattered image of in-situ synthesized 40:60(LSMO: NFO) composite; also the EDAX.

The Fig 4.2.2 (c), (d) shows the surface topology of 40LSMO: 60NFO; the magnification was maintained at 5,000 at 15kV. From the EDAX of 40:60 we can observe that the bright contrast is LSMO and dark contrast is NFO.

### 4.2.3 Density

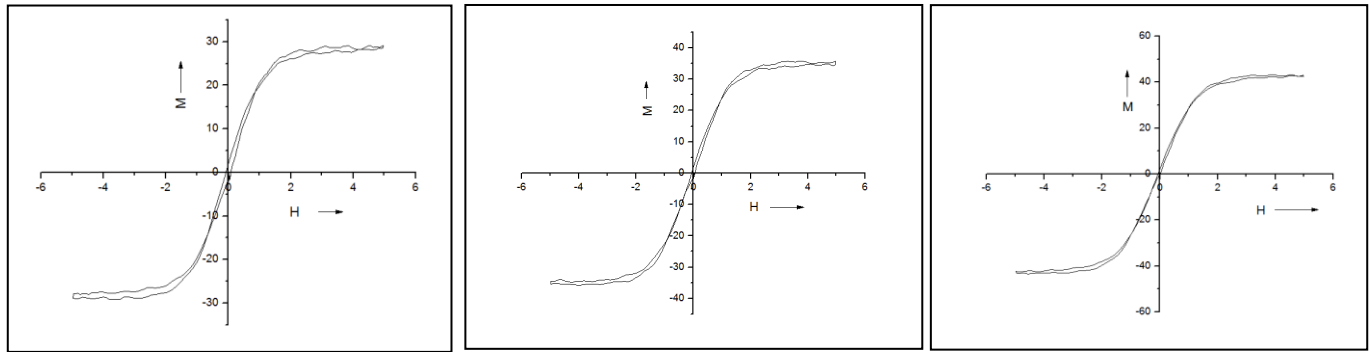
Table 4.1 shows the bulk density(B.D) and apparent porosity(A.P) of in-situ synthesized composites, those are sintered at 1200 °C.

Table 4.1: shows the values of Bulk density and apparent porosity of in-situ samples.

Serial No.	Sample (NFO:LSMO)	Bulk density (g/cc)	Apparent porosity (%)
1	50:50 (IS*)	4.52	20.3
2	60:40 (IS)	5.00	16.5
3	80:20 (IS)	5.45	13.4

### 4.2.4 Magnetic hysteresis loop

Figure 4.2.3 (a),(b),(c) shows the hysteresis loop of in-situ synthesized composite sintered at temperature 1200 °C of composition 50:50(LSMO:NFO),60:40,80:20 respectively.



(a)

(b)

(c)

Fig 4.2.3: MH loop (a) 50 LSMO: 50 NFO, (b) 40 LSMO: 60 NFO, and (d) 20 LSMO:80 NFO samples

It can be clearly seen that the disturbances in the curves are decreasing from figure (a) to(b) to(c).This is because of the NFO content in the samples are increasing and there for it shows better magnetic properties along with a well defined magnetic hysteresis loop Table 4.5.

#### 4.2.5 Remarks

From the DSC-TG we can infer that the calcine temperature of in-situ synthesized composition (40LSMO:60NFO,20LSMO:80NFO,50LSMO:50NFO)is around 800 – 1000 °C.The bulk density of the in-situ are almost similar to each other and the value is around  $\sim 5 \text{ g/cm}^3$ .As the percentage of NFO varies, a variation the hysteresis loop can be observed; the amount of distortion in the hysteresis keeps on decreasing as we decrease the percentage of LSMO.This helps in deciding the percentage of LSMO and NFO for a required material with a given specification.

### 4.3 Characterization of LSMO: $\text{NiFe}_2\text{O}_4$ composites by solid-state route

#### 4.3.1 Structure and microstructure

The presence of phases and the crystallite size was calculated from the X-ray diffraction pattern. Figures 4.2.2 (a), (b),(c) shows the XRD graphs of in-situ synthesized composites with composition50:50 (LSMO: NFO) 40:60(LSMO:NFO)and 20:80 (LSMO: NFO) respectively. All the peaks are identified to either NFO or LSMO without impurities.

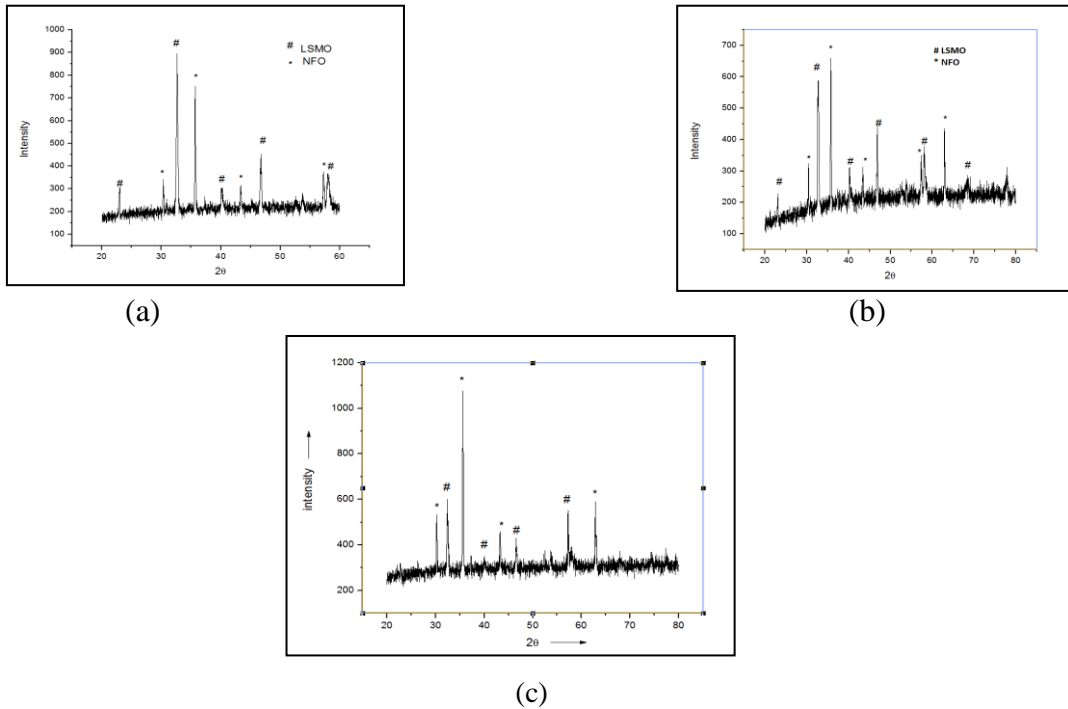


Fig 4.3.1: XRD pattern of (a) 50 LSMOs: 50NFO, (b) 40 LSMO: 60 NFO and (c) 20 LSMO: 80 NFO

Figures 4.3.1 (c), (d) shows the secondary electron image and back scattered image of solid route synthesized 20:80(LSMO: NFO) composites.

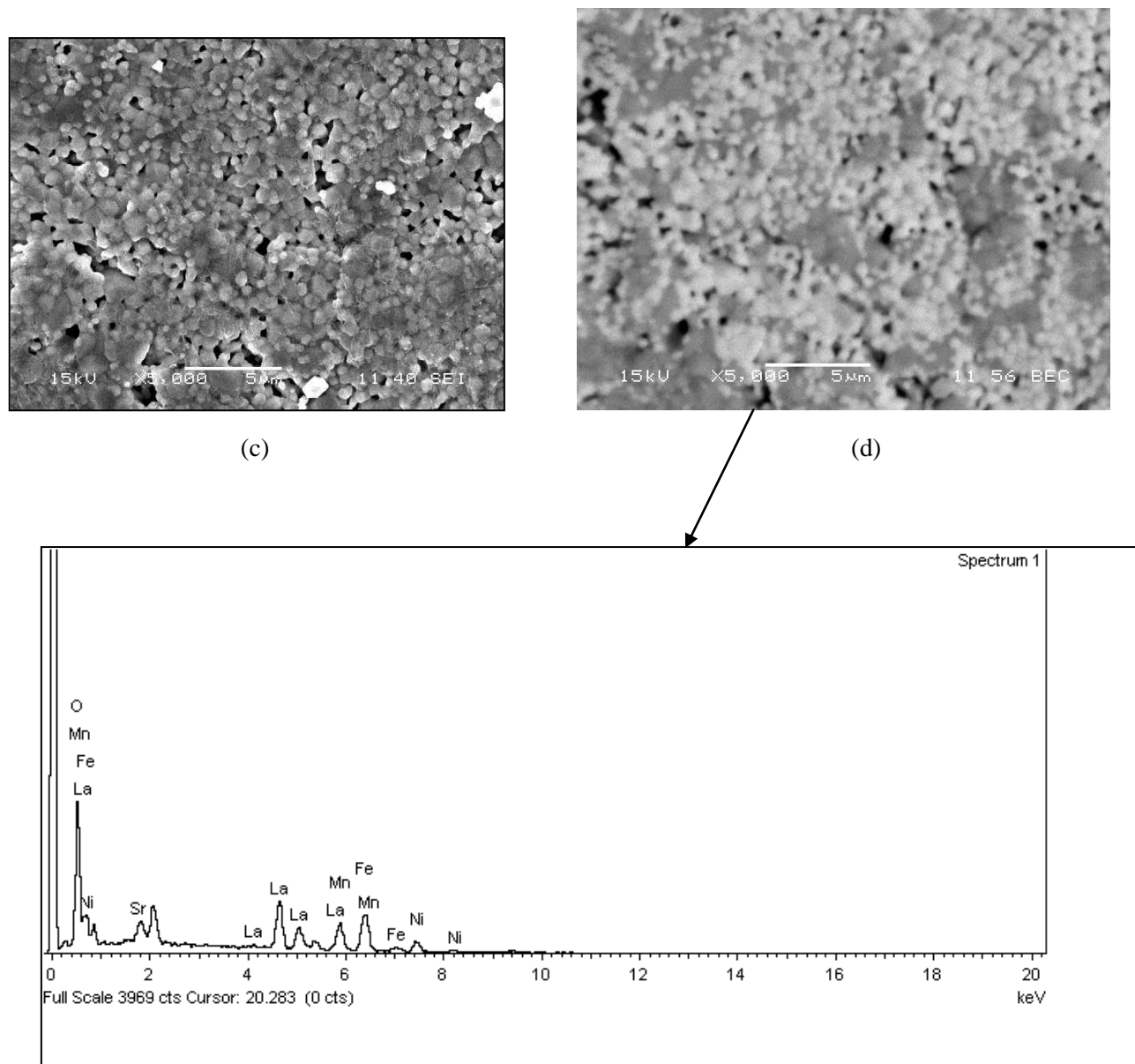


Fig 4.3.1: SEM image of (c) 60:40(Secondary Electron image), (d) 60:40 (backscattered electron image) showing EDAX.

The crystallite size of LSMO and NFO was found to be around 45 nm and 70 nm, respectively. The Fig 4.3.1 (c), (d) shows the topography of solid route synthesized sample, the image shows that the porosity level in this sample are much more than in-situ route prepared sample. The BSE

image shows the presence of two phases in the sample and it can be seen from the EDAX of whole surface. From the EDAX it can be inferred that percentage of NFO and LSMO is around 66.37: 33.63 respectively.

#### 4.3.2 Density

Table 4.2 shows the bulk density(B.D) and apparent porosity(A.P) of in-situ synthesized composites, those are sintered at 1200 °C.

Table 4.2: Bulk density and apparent porosity of solid route synthesized samples

Serial No.	Sample (LSMO:NFO)	Bulk density (g/cc)	Apparent porosity (%)
1	20:80(SS*)	4.16	28.03
2	40:60(SS)	4.11	20.79
3	50:50(SS)	4.70	21.32

Table 4.3 shows the bulk density(B.D) and apparent porosity(A.P) of different synthesized sample, with different composition and different routes.

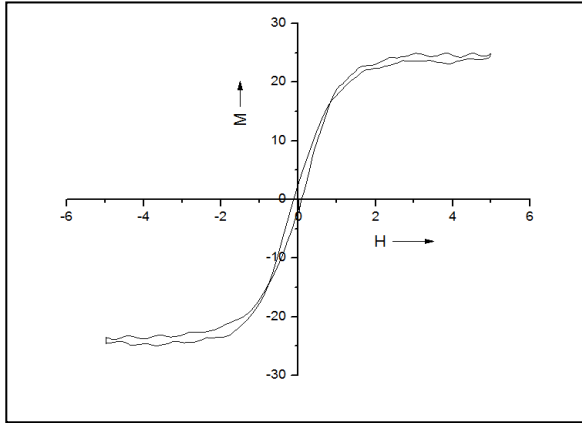
Table 4.3: Bulk density and apparent porosity synthesized samples

Serial No.	Sample (LSMO:NFO)	Dry weight (D) g	Soaked weight (W)g	Suspended Weight (S)g	Bulk density (g/cc)	Apparent porosity (%)
1	20:80(SS*)	0.6048	0.6373	0.5196	4.16	28.03
2	40:60(SS)	0.5802	0.6142	0.5001	4.11	20.79
3	50:50(SS)	0.6447	0.6684	0.5573	4.70	21.32
4	50:50(IS*)	0.6209	0.6488	0.5377	4.52	24.97
5	40:60(IS)	0.5746	0.6030	0.4923	3.83	25.65
6	20:80(IS)	0.6023	0.6449	0.5462	4.94	43.16
7	NFO(IS)	0.6023	0.6449	0.5150	3.75	32.79
8	LSMO(IS)	0.5233	0.5485	0.4492	4.26	25.07

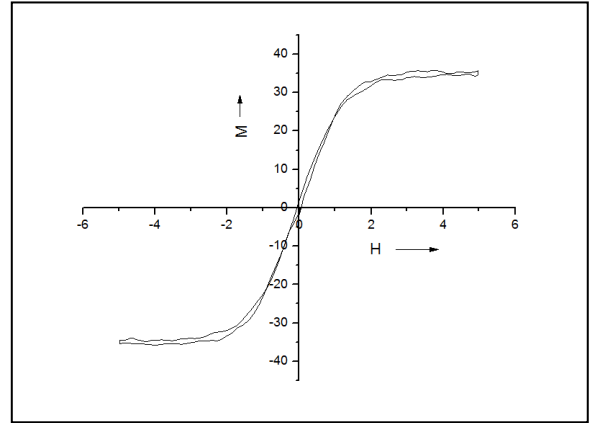
SS\*=solid state route, IS\*=in-situ route

### 4.3.3 Magnetic hysteresis loop

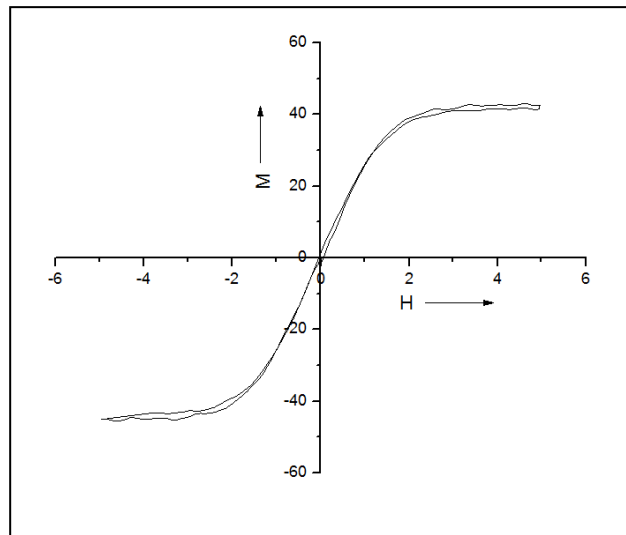
Figure 4.3.2 (a), (b) and (c) shows the hysteresis loop of solid route synthesized composites at temperature 1200 °C of composition 50:50(LSMO: NFO), 40:60, 20:80 respectively.



(a)



(b)



(c)

Fig 4.3.2: Magnetic Hysteresis loop (a) 50:50, (b) 40:60, and (d) 20:80



It can be clearly observed in the above M-H diagrams that as the NFO concentration increases the disturbances in the M-H loop also decrease. This shows that there is an improvement in the magnetic properties of the samples as the concentration of NFO is increasing. There is no significant difference between the M-H curves of samples prepared by insitu process and samples prepared by solid state process.

Table 4.4: shows the values for Coercive Field ( $O_c$ ), Remanent magnetization ( $M_r$ ) in emu/g, Saturation magnetization ( $M_s$ ) in emu/g in different composition of LSMO and NFO, prepared by different routes.

Composition	Process	$M_s(\text{emu/g})$	$M_r(\text{emu/g})$	$H_c$
NFO	In-situ	52.7	0.5439	3.34
LSMO	In-situ	****	****	****
50:50	Solid-solid	24.9901	2.3675	102.5324
50:50	In-situ	29.1691	0.225	58.503
20:80	Solid-solid	42.999	0.2872	36.4346
20:80	In-situ	43.489	-0.154	18.8542
40:60	Solid-solid	38.555	0.548	23.845
40:60	In-situ	35.773	13.635	43.645

#### 4.2.4 Remarks

The solid state synthesis involved mixing and grinding of samples with the help of mortar pestle. This kind of grinding and mixing affects the phase distribution and porosity of the sample. The variation in magnetic behavior was observed with decreasing amount of LSMO, the distortion in the M-H loop kept on decreasing. The SEM images shows the percentage of porosity is much higher than that of in-situ synthesized sample, the dark contrast and the bright contrast is of NFO and LSMO respectively.

# Chapter 5

**CONCLUSIONS**

The findings of the present work are summarized below:

- (1) The NFO: LSMO composites were successfully prepared with the help of microwave assisted insitu process and solid state process. The characterizations on the prepared samples were also done.
- (2) The porosity of the prepared sample was calculated. It was observed that the calculated apparent porosity values of the solid route samples were lower than the apparent porosity values of the solid state samples.
- (3) SEM images were studied carefully and it was observed that the bright part refers to LSMO and the dark part refers to NFO.
- (4) The M-H curve was studied and it can be concluded that as the amount of NFO in the samples are increasing the amount of disturbances in the curve decreases or the curve becomes smooth. So, it can be said that on increasing the amount of NFO in the samples the magnetic properties can be improved.

.

## REFERENCES:

- 1.T. Tang, S. Y. Zhang, R. S. Huang, and Y. W. Du, *J. Alloys and Comp.*, **353**, (2003) 91.
- 2.B.B. Nayak, S. Vitta, A.K. Nigam, D. Bahadur, *Mater. Sci. Eng. B* **113** (2004) 50.
- 3.Q. Huang, J. Li, X. Huang, C. K. Ong, and X. S. Gao, *J. Appl. Phys.*, **90** (2001) 2924.
- 4.C.-H. Yan, Z.-G. Xu, T. Zhu, Z.-M. Wang, F.-X. Cheng, Y.-H. Huang, and C.-S. Liao, *J. Appl. Phys.*, **87** (2000) 5588.
- 5..C. Zener, *Phys. Rev.*, **82** (1951) 403.
- 6.M. W. Barsoum, “Fundamentals of Ceramics”, IOP publishing, Bristol and Philadelphia, 2003 page-530
7. K.P. Lim, K.P. Lim, S.W. Ng, S.A. Halim, S.K. Chen and J.K. Wong, *J. Applied Sci.*, **6** (2009) 1153-1157.
8. L.E. Huesoa, J. Rivasa, *Journal of Non-Crystalline Solids*, **324-328**(2001)287.
- 9.Shilpi Karmakar<sup>1</sup>, S Taran<sup>1</sup>, B K Chaudhuri<sup>1,3</sup>, H Sakata<sup>2</sup>, C P Sun<sup>3</sup>, C L Huang<sup>3</sup> and H D Yang<sup>3</sup>, *\*Journal of Physics D: Applied Physics*, **20**,(2005)38.
- 10.Sudipta Pal<sup>1</sup>, Aritra Banerjee<sup>1</sup>, S. Chatterjee<sup>2</sup>, A. K. Nigam<sup>2</sup>, B. K. Chaudhuri<sup>1</sup>, and H. D. Yang<sup>3</sup>. *J. Appl. Phys.* 94, (2003) 3485.
- 11 .Huang, Q.; Li, J.; Huang, X. J.; Ong, C. K.; Gao, X. S.; *Journal of Applied Physics*, **90**(2009).
- 12.Sayani Bhattacharyaa, Sudipta Pala, R. K. Mukherjeea, B. K. *Journal of Magnetism and Magnetic Materials*,**359-371** (2004) 269.
- 13.Das, D.; Saha, A.; Russek, S. E.; Raj, R.; Bahadur, D.;*Journal of applied physics*,(2003)93.
- 14.A. Maignan\*, C. Martin, F. Damay, and B. Raveau, *Phys. Rev. B* **58**, (1998), 2758–2763.
- 15.E. O. Wollan and W. C. Koehler . *Phys. Rev.* **100**, (1955), 545–563